Frontal eye field microstimulation induces task-dependent gamma oscillations in the lateral intraparietal area

Elsie Premereur, Wim Vanduffel, Pieter R. Roelfsema and Peter Janssen

J Neurophysiol 108:1392-1402, 2012. First published 6 June 2012; doi:10.1152/jn.00323.2012

J Neurophysiol 108: 1392–1402, 2012.
First published June 6, 2012; doi:10.1152/jn.00323.2012.

Frontal eye field microstimulation induces task-dependent gamma oscillations in the lateral intraparietal area

Elsie Premereur,[1] Wim Vanduffel,[1,2,3] Pieter R. Roelfsema,[4,5] and Peter Janssen[1]

[1]*Laboratorium voor Neuro- en Psychofysiologie, Katholieke Universiteit Leuven, Leuven, Belgium;* [2]*Athinoula A. Martinos Center for Biomedical Imaging, Massachusetts General Hospital, Charlestown, Massachusetts;* [3]*Department of Radiology, Harvard Medical School, Boston, Massachusetts;* [4]*Netherlands Institute for Neuroscience, Amsterdam, The Netherlands; and* [5]*Department of Integrative Neurophysiology, Centre for Neurogenomics and Cognitive Research, VU University, Amsterdam, The Netherlands*

Submitted 19 April 2012; accepted in final form 5 June 2012

Premereur E, Vanduffel W, Roelfsema PR, Janssen P. Frontal eye field microstimulation induces task-dependent gamma oscillations in the lateral intraparietal area. *J Neurophysiol* 108: 1392–1402, 2012. First published June 6, 2012; doi:10.1152/jn.00323.2012.—Macaque frontal eye fields (FEF) and the lateral intraparietal area (LIP) are high-level oculomotor control centers that have been implicated in the allocation of spatial attention. Electrical microstimulation of macaque FEF elicits functional magnetic resonance imaging (fMRI) activations in area LIP, but no study has yet investigated the effect of FEF microstimulation on LIP at the single-cell or local field potential (LFP) level. We recorded spiking and LFP activity in area LIP during weak, subthreshold microstimulation of the FEF in a delayed-saccade task. FEF microstimulation caused a highly time- and frequency-specific, task-dependent increase in gamma power in retinotopically corresponding sites in LIP: FEF microstimulation produced a significant increase in LIP gamma power when a saccade target appeared and remained present in the LIP receptive field (RF), whereas less specific increases in alpha power were evoked by FEF microstimulation for saccades directed away from the RF. Stimulating FEF with weak currents had no effect on LIP spike rates or on the gamma power during memory saccades or passive fixation. These results provide the first evidence for task-dependent modulations of LFPs in LIP caused by top-down stimulation of FEF. Since the allocation and disengagement of spatial attention in visual cortex have been associated with increases in gamma and alpha power, respectively, the effects of FEF microstimulation on LIP are consistent with the known effects of spatial attention.

saccades; spatial attention; macaque

ATTENTION ENHANCES the relevant signals among the flood of information entering the eye (Desimone and Duncan 1995; Reynolds and Chelazzi 2004). Previous work implicated saccade-related areas in spatial attention (Corbetta et al. 1998; Gattass and Desimone 1996; Kustov and Robinson 1996; Petersen et al. 1987; Rizzolatti et al. 1987), but little is known about the functional interactions between high-level oculomotor areas. Two main structures involved are the macaque frontal eye fields (FEF) and the lateral intraparietal area (LIP). Area LIP contains neurons that discharge before and during saccadic eye movements, and electrical stimulation of LIP evokes saccades (Thier and Andersen 1998). Furthermore, LIP activity can be modulated by selective attention (Colby et al. 1996), and reversible inactivation of area LIP causes a deficit in covert visual attention (Liu et al. 2010; Wardak et al. 2004). The FEF is also involved in the control of voluntary saccades (Bruce et al. 1985; Schall 1995; Tehovnik et al. 2000), since electrical microstimulation of the FEF evokes highly reproducible contralateral eye movements. Furthermore, stimulating FEF at a current level below the threshold for evoking saccades causes attention-like effects both behaviorally (Moore and Fallah 2001) and on the neural activity in area V4 (Moore and Armstrong 2003). Covert attention is also associated with enhanced oscillatory coupling between FEF and V4 initiated by FEF, suggesting that FEF is a source of the attentional effects on gamma synchrony in V4 (Gregoriou et al. 2009).

Anatomical studies have shown reciprocal connections between the FEF and LIP (Anderson et al. 2011; Huerta et al. 1987; Schall et al. 1995; Stanton et al. 1995), and the areas share many neuronal characteristics. Furthermore, imaging studies have shown the activation of a frontoparietal network during attention tasks (Corbetta et al. 1998; Nobre et al. 2000; Wardak et al. 2010), and FEF microstimulation causes enhanced functional magnetic resonance imaging (fMRI) activation in LIP, even in the absence of visual stimulation (Ekstrom et al. 2008). However, no study has investigated the effect of FEF on LIP at the level of the single cell and local field potentials (LFPs). Therefore the goal of our study was to investigate the effects of subthreshold FEF stimulation on LIP under different task conditions. We found that FEF microstimulation elicits highly time- and frequency-specific, task-dependent effects on retinotopically corresponding sites in area LIP: FEF microstimulation caused a significant increase in the low-gamma power of the LFP in LIP when a salient saccade target appeared in the receptive field (RF) but not when a distractor appeared in the RF. In contrast, when the saccade target appeared outside the LIP RF, FEF microstimulation elicited an enhancement in alpha power in area LIP. Increases in gamma power have been associated with the allocation of spatial attention (Fries et al. 2001), while increased alpha power has been associated with disengagement of spatial attention (Worden et al. 2000). Thus FEF selectively modulates activity in LIP at the level of the LFP, consistent with the known effects of spatial attention.

Address for reprint requests and other correspondence: P. Janssen, Katholieke Universiteit Leuven, O&N 2, Laboratorium voor Neuro- en Psychofysiologie, Herestraat 49, Bus 1021, 3000 Leuven, Belgium (e-mail: peter.janssen@med.kuleuven.be).

MATERIALS AND METHODS

Subjects and Surgery

All experiments were performed on two juvenile male rhesus monkeys (*monkey Tm*, 4 kg; *monkey Tb*, 6 kg). After the monkeys were trained to sit in a primate chair, a custom-made head post was implanted on the skull with ceramic screws and dental acrylic. At least 6 wk after surgery, the monkeys began training in passive fixation and eye movement tasks. After 2–4 mo of training, 43 platinum-iridium wire electrodes (Teflon-coated microwire, 25-μm diameter, 90% platinum, 10% iridium) were chronically implanted in area FEF in the left hemisphere, along the rostral bank of the arcuate sulcus, at a depth of 3–5 mm (Fig. 1*A*, *top*; see Ekstrom et al. 2008). Note that we do not know the position and depth of individual electrodes. Because of the chronic implantation, the current levels required to elicit saccades are higher than in acute experiments (Ekstrom et al. 2008, 2009) and cannot be used to infer the depth of the electrode (Stanton et al. 1989). Wire tips were stripped of ~40 μm of Teflon prior to insertion. Three electrodes were implanted between skin and muscle and served as ground. Electrodes were connected with a magnetic resonance imaging (MRI) magnet-compatible connector (Omnetics) and typically had impedances in the range of 5–200 kΩ.

Three to four weeks after electrode implantation, a craniotomy was made over the lateral bank of the intraparietal sulcus (IPS), and a MRI-compatible recording cylinder (Crist Instrument) was implanted at an oblique angle parallel with respect to the IPS (Fig. 1*A*, *bottom*). Note that the oblique approach prevented us from accurately estimating the layers we recorded from. All surgeries were performed under isoflurane anesthesia and sterile conditions. Recording cylinders were implanted over the left hemisphere (Horsley-Clark coordinates 10–11P and 14–18L). To verify the recording positions, we inserted glass capillaries filled with a 2% copper sulfate solution into the recording grid (Crist Instrument) at several grid positions, acquired structural MR images (0.6-mm resolution), and reconstructed the electrode penetrations with BrainSight (Rogue Research). All procedures were performed in accordance with the National Institutes of Health *Guide for the Care and Use of Laboratory Animals* and were approved by the Ethical Committee at the Katholieke Universiteit Leuven Medical School.

Stimuli and Tests

All stimuli were displayed on a Philips Brilliance 202P4 CRT monitor operating at 120 Hz at a viewing distance of 86 cm.

Visually guided saccade task with multiple distractors. Spiking and LFP activity were recorded during a visually guided saccade task with multiple distractors (Premereur et al. 2011), in which the animal has to divide its attention over the target and the distractors. Previous research has shown that the effects of both spatial attention and FEF stimulation are largest in the presence of multiple distractors (Ekstrom et al. 2008; Moore and Armstrong 2003; Reynolds et al. 1999). During the visually guided saccade task with multiple distractors, monkeys had to maintain fixation within a window of $<2° \times 2°$ around a small red spot in the center of the display for a fixed duration of 450 ms, after which a single green saccade target and four gray distractors would appear (Fig. 1*C*). Target and distractors were equal in size

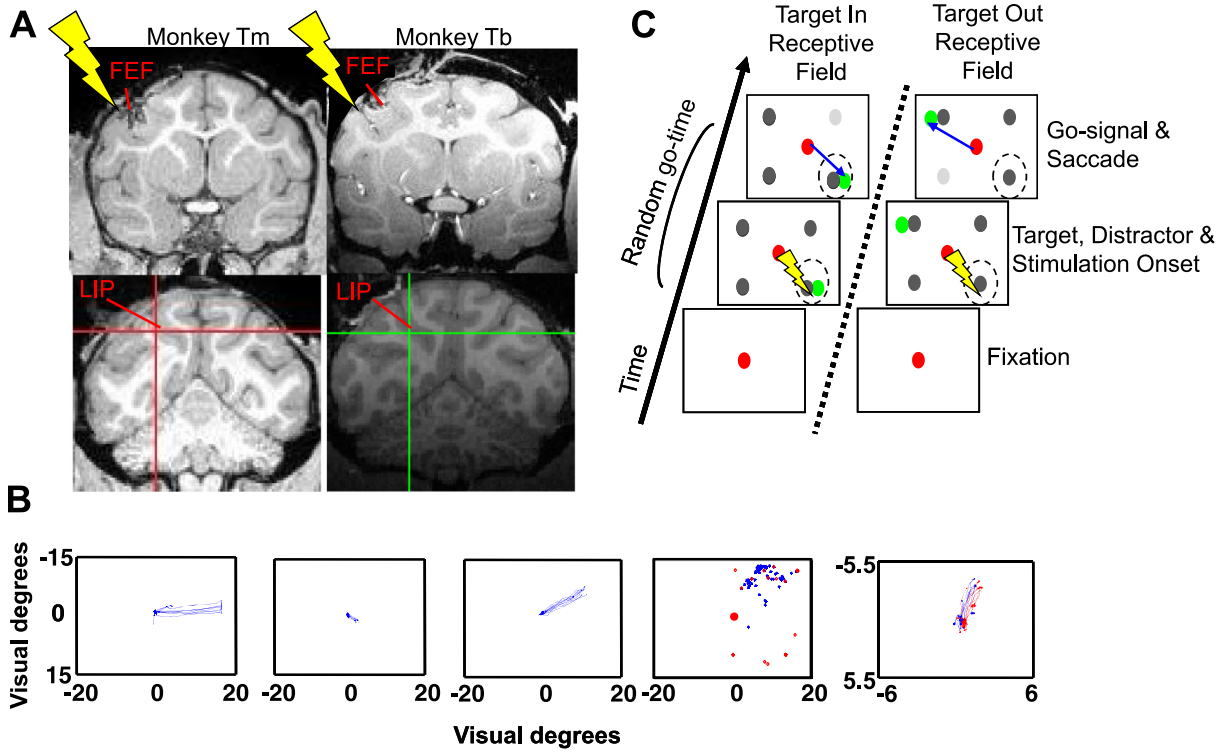

Fig. 1. Recording area and task. *A*, *top*: anatomical MRI (T1-weighted MPRAGE) showing the frontal eye field (FEF) stimulation electrodes (Horsley-Clark coordinates: 18 anterior, 18 lateral). *Bottom*: coronal MR images showing representative lateral intraparietal area (LIP) recording sites in both monkeys. *B*: example saccade vectors. Black boxes represent screen size; blue traces show eye traces evoked by suprathreshold FEF microstimulation of 3 different electrodes. The 4th panel shows the end points of all saccade vectors used in our experiment. Central red dot, fixation point; blue dots, end points of saccade vectors used in experimental sessions; red diamonds, end points of saccade vectors used in control sessions. Last panel shows saccades evoked with typical parameters (blue traces: 200 Hz, 0.4-ms pulse width) and with our parameters (red traces: 100 Hz, 0.16-ms pulse width). *C*: visually guided saccade task with multiple distractors. After a fixed period of fixation, 4 gray distractors and 1 green saccade target appeared. The target was either positioned inside the LIP receptive field (RF) (dotted circle, *left*) or on the contralateral side (*right*). FEF stimulation started simultaneously with target onset, and the saccade vector was directed toward the RF (indicated by lightning symbol). After a random period of fixation, 1 of the distractors brightened, indicating to the monkey to make a saccade to the green target (represented by arrow).

(0.25°) and luminance (6 cd/m^2). The saccade target appeared either in the LIP RF (Target-In condition) or at the opposite position, ipsilateral to the recording cylinder (Target-Out condition). The distractors appeared in the upper and lower hemifield ipsilateral and contralateral to the RF, one of them always appearing inside the RF (Fig. 1*C*). After a variable delay (between 500 and 2,000 ms), the luminance of one of the distractors (selected at random) increased by 300%, instructing the animal to saccade to the green target. The monkey was rewarded for making a saccade toward the target within 500 ms after the go signal (i.e., the brightening of 1 of the distractors) and holding fixation within a 3–4° window around the target for 250 ms. Because the go signal could appear at any of the four distractor locations, the animal had to covertly attend to all four locations on the display. To encourage fast responses, reward size was governed by an exponential function of the reaction time (RT) between 150 and 500 ms after the go signal. The time (t) between target onset and the go signal was a random variable drawn from a unimodal Weibull distribution delayed by 500 ms (Janssen and Shadlen 2005):

$$U(t) = \begin{cases} 3\alpha(t - 1/2)^2 e^{-\alpha(t - 1/2)^3} & \text{for } t > 1/2 \\ 0 \text{ otherwise} \end{cases} \quad (1)$$

In half of the trials, one FEF electrode was stimulated at one-third of the saccade threshold (frequency 100 Hz; pulse width 0.16 ms; biphasic square-wave pulse, 0.08 ms pos, 0.08 ms neg). For the experimental recording sites, the FEF saccade vector was directed toward the LIP RF. Stimulation started simultaneously with target onset and lasted for 500 ms. Thus, importantly, FEF stimulation always stopped before the go signal could appear. More exactly, in the majority of the trials (93%), the go signal occurred >200 ms after the end of FEF stimulation. In the control experiments, the direction of the FEF saccade vector was directed away from the LIP RF and toward the distractor that was located in the same hemifield as the LIP RF.

Memory-guided saccade task. A green saccade target appeared for a period of 200 ms after 450 ms of fixation, inside or outside the RF. After disappearance of the target, the monkey had to maintain central fixation until the fixation point dimmed, thereby cuing the animal to saccade to the remembered target position. The saccade target was presented inside the RF or at the opposite position. Timing of the go signal and stimulation parameters were identical to the multiple distractor task.

Passive fixation task. After an 800-ms period of fixation, a colored static grating (1.5° in diameter) was presented for 600 ms in the RF in 80% of the trials. In interleaved trials, no visual stimulus was presented but timing parameters were equal to trials in which a grating was presented. The monkeys were required to keep fixating until 500 ms after stimulus offset, at which time a reward was administered. Stimulation started at distractor onset or at equivalent times in the no-grating trials. Stimulation parameters were identical to those used in the multiple distractor saccade task.

The three tasks were presented in blocks of 80–120 trials, with multiple repetitions if possible.

Recording and Stimulation Techniques

The position of the right eye was recorded at a sampling rate of 500 Hz with an EyeLink 1000 eye tracker (SR Research). A photocell was attached to the monitor to detect the onset of a white square in the lower right corner of the screen (covered with black tape to obscure it from the monkeys' view) that appeared in the first video frame containing a stimulus (distractor, saccade target, or go signal). For every recording session, a tungsten microelectrode (impedance at 1 kHz: 0.8–1.2 MΩ; FHC) was inserted with a hydraulic microdrive (FHC) through a stainless steel guide tube in a plastic grid (spacing 1 mm; Crist Instrument). Spiking activity was amplified (Bak Elektronics) and filtered between 300 and 5,000 Hz (Wavetec Filter; TekNet Electronics), LFP activity was filtered between 1 and 170 Hz (Frequency Devices). Eye position signals, neural activity, photocell pulses, and stimulation pulses were digitized and processed at 20 kHz on a digital signal processor (DSP) (C6000 series; Texas Instruments) and saved at 1 kHz (spike signal at 20 kHz). The onset of the stimulation signal was controlled by custom-made software (LabVIEW, National Instruments) that also controlled the visual stimulation.

At the beginning of every recording session, FEF electrodes were tested to determine the saccade vector and the minimum voltage necessary for evoking saccades. Monkeys performed a passive fixation task while voltage was administered by means of an eight-channel Digital Stimulator (DS8000, WPI). Stimulation trains for evoking saccades lasted for 200 ms (pulse width 0.48 ms, 100 Hz) and consisted of biphasic square-wave pulses. Stimulation threshold was determined as the minimum current necessary for generating a saccade and was typically in the range of 60–200 μA. Note that the saccade thresholds described in this experiment are higher than typically described in FEF stimulation experiments, most likely because of the chronic implantation (causing growth of a fibrous barrier between the electrodes and neural tissue; see also Ekstrom et al. 2008) and the blunt tips of the electrodes. The saccadic end points we evoked by FEF microstimulation ranged from +13° to −14° in the vertical direction and from 0° to 18° in the horizontal direction (Fig. 1*B*).

During the recordings, the pulse width was reduced to 0.16 ms (biphasic square-wave pulse, 0.08 ms pos, 0.08 ms neg) and one-third of the saccade threshold. Importantly, stimulating FEF at 100 Hz and 0.16-ms pulse width could evoke saccades in the majority of the FEF electrodes (data not shown). Furthermore, we verified for two other monkeys with chronically implanted FEF electrodes that saccades could be evoked with our parameters, using currents similar to those necessary for evoking saccades with standard parameters (200 Hz, 0.4-ms pulse width. Fig. 1*B*, last panel). Previous research has also determined that saccades can be evoked by FEF stimulation with parameters similar to those we used (i.e., 150 Hz, 400-ms stimulation, single pulse width 0.1 ms) at currents of 50–200 μA and that the frequency of FEF stimulation did not affect the probability to evoke saccades (Tehovnik and Sommer 1997).

Our stimulation parameters were selected on the basis of ability to record action potentials between stimulation pulses: since each 0.16-ms stimulation pulse caused an electronic artifact of typically 1.5–2.5 ms, only 15–25% of the signal could not be used for spike detection at 100 Hz. At half of the saccade threshold with a pulse width of 0.48 ms, the stimulation artifact would typically increase to 4–5 ms, allowing us to use only 50–60% of the spike signal for off-line spike sorting (see *Stimulation Artifact Removal*).

In a typical recording session, the electrode was lowered into the lateral bank of the IPS while the monkey made delayed visually guided saccades. We searched for responses in multiunit activity (MUA) by placing saccade targets at various locations in the contralateral hemifield. LIP neurons were not screened for delay activity during memory-guided saccades; the only inclusion criterion was spatially selective saccadic activity (Premereur et al. 2011). All recording sites were located in the lateral bank of the IPS in the vicinity (<2 mm) of sites with memory-delay activity.

Formal testing started once a spatially selective multiunit or single-unit target response was observed. If the LIP RF was aligned with the saccade vector of one of the chronically implanted FEF electrodes, an experimental session was started; otherwise the saccade target was positioned inside the LIP RF, and one of the four distractors was positioned in the FEF movement field (MF) to carry out a control experiment.

Stimulation Artifact Removal

To limit the size of the stimulation-induced electronic artifact, FEF was stimulated at one-third of the saccade threshold, at 100 Hz and with narrow stimulation pulses (0.16-ms pulse width). Furthermore, we removed 1.5–2.5 ms of the raw filtered spike signal after every stimulation pulse (depending on the width of the stimulation artifact; 15–25% of the signal for a 100-Hz stimulation frequency) with custom-designed software (LabVIEW, National instruments) by replacing the values of the continuous spike signal during this interval by the value obtained immediately before the stimulation pulse (see Fig. 4*B*, *inset*). The same procedure was employed in the no-stimulation trials based on stimulation time stamps extracted from the stimulation trials. The signal obtained was used for off-line spike sorting (Plexon Offline Sorter; template matching).

Stimulating FEF at 100 Hz caused an artifact in the LFP recordings that was visible as an increase in power in the LFP power spectrum around 100 Hz in all conditions. To exclude the possibility that any changes in the power spectrum were obtained because of the stimulation artifact, we excluded the power spectrum above 80 Hz from all analyses. To verify that the artifact caused by FEF microstimulation was restricted to the LFP frequency bands around 100 Hz, we also investigated the effect on frequency bands above 120 Hz and found no increase in power in stimulation trials. Therefore FEF stimulation only causes an electrically induced increase in power around 100 Hz.

Data Analysis

All LFP data were analyzed with the Morlet's wavelet analysis technique (Tallon-Baudry and Bertrand 1999) with a spectro-temporal resolution of 7, after filtering with a 50-Hz notch filter. This method provides a better compromise between time and frequency resolution compared with methods using Fourier transforms (Sinkkonen et al. 1995; Tallon-Baudry et al. 1997). To exclude trials with possible artifacts in the LFP recordings, maximum and minimum values of the continuous LFP signal and of the time-frequency spectrum were calculated per trial and trials with minimum values below the 5th percentile and maximum values above the 95th percentile were removed. Furthermore, the data set was split in two, and all population analyses were repeated for both halves of the population of recording sites to check for consistency. If inconsistent findings were found because of one trial/recording site with extreme values, this trial/recording site was removed. We analyzed the LFP power in standard frequency bands: medium gamma (50–80 Hz), low gamma (25–50 Hz), beta (12–25 Hz), and alpha (8–12 Hz). Frequencies above 80 Hz were excluded from our analyses to avoid any possible influence of an electrically induced stimulation artifact. LFP power was averaged across trials and over frequencies to extract the average power per frequency band over time. Visual inspection of the time-frequency spectrogram showed that none of the results was due to effects in one specific frequency: effects were present throughout all frequencies in a specific band. LFP data were not corrected for average visually evoked potentials (VEPs), but removing the VEP yielded similar response patterns. LFP analyses using multitaper methods also revealed similar results.

Power was normalized per trial by dividing the power trace per frequency by the average power for this frequency in the 300-ms interval before stimulus onset. All statistics on the LFP data (0–500 ms after stimulus onset) were performed with permutation tests, where actual data (obtained in the overall data set, $n = 16{,}668$ trials) were randomly divided over all the various conditions 10,000 times, and the differences between two conditions were calculated for every permutation, to compare with the actual difference between conditions. We also calculated permutation tests on the data obtained in each monkey separately ($N = 14{,}155$ trials in *monkey Tb*, $N = 2{,}513$ in *monkey Tm*).

Spike-field coherence (SFC) was calculated between single-unit activity (SUA) and LFP activity recorded with the same electrode with the Chronux toolbox (**http://chronux.org/**) (Bokil et al. 2010). Only SUA sites were included, as our artifact removal technique did not allow us to distinguish the remaining stimulation artifact from MUA activity. For coherence analysis, only trials with a go time of 900 ms or longer were included. LFP data were corrected for the average VEP by trialwise subtraction of the average VEP for a given site and condition. We calculated the temporal dynamics of the average SFC after target onset in the same frequency bands as for the LFPs, in time bins of 350 ms with a 10-ms step width. Differences between conditions were tested for significance with permutation tests in the interval 0–900 ms. Increases in coherence after stimulus onset were tested for significance with nonparametric permutation tests by comparing baseline coherence (−300 to 0 ms) with coherence in the 0–200 ms interval. Time bandwidth product and number of tapers were set at 3 and 5, respectively. We randomly extracted the same number of trials for every condition.

Spike rate analyses. To avoid any possible influence of go signal or saccade execution, the average spike rate was plotted aligned on target onset and only up to 50 ms after the go signal (bin width 80 ms). Tests for significant differences between conditions were performed with *t*-statistics on the average activity between 0 and 500 ms after stimulus onset.

Reaction time. RT was defined as the point in time when the velocity of the eye trace exceeded five times the standard deviation of the velocity in the interval from 700 until 100 ms before the go signal (typically in the range of 120–170°/s).

RESULTS

Two rhesus monkeys were chronically implanted with platinum-iridium wire electrodes in the FEF of the left hemisphere (Fig. 1*A*, *top*). We recorded spatially selective saccadic SUA, MUA, and LFP activity in area LIP of the same hemisphere (Fig. 1*A*, *bottom*). At the beginning of every recording session, the saccadic vectors and thresholds of the FEF electrodes were determined (Fig. 1*B*). Note that the vectors were consistent across sessions (Fig. 1*B*, 4th panel). Neural activity was recorded during a visually guided saccade task with multiple distractors (Fig. 1*C*) in which the saccade target (distinguished by its color) was positioned either inside the LIP RF or at the opposite location (Fig. 1*C*) and the FEF saccade vector was aligned with the LIP RF. One distractor was always positioned inside the RF, and the remaining distractors were positioned in the three other quadrants. The dimming of one of these distractors served as the go signal during the saccade task. Subthreshold FEF microstimulation (1/3 of the saccade threshold; pulse width = 0.16 ms; frequency = 100 Hz, duration: 500 ms) was initiated at stimulus onset. We stimulated FEF with weak stimulation parameters compared with previous research (Ekstrom et al. 2008; Moore and Armstrong 2003) because this allowed us to measure the effect of FEF microstimulation on LIP activity during the stimulation interval itself (higher FEF currents induced a stronger electrical artifact, which prevented any analysis of LFPs or spikes during the stimulation interval). We recorded LIP activity during FEF microstimulation from sites showing spatially selective saccadic activity in either SUA or MUA (*monkey Tm*: $N = 20$; *monkey Tb*: $N = 66$).

Figure 2*A* shows the time-frequency spectrum of the LFP in an example site in the absence of microstimulation ($n = 62$ trials). Stimulus onset in the RF evoked a robust increase in gamma power (25–170 Hz) that was significantly stronger in trials

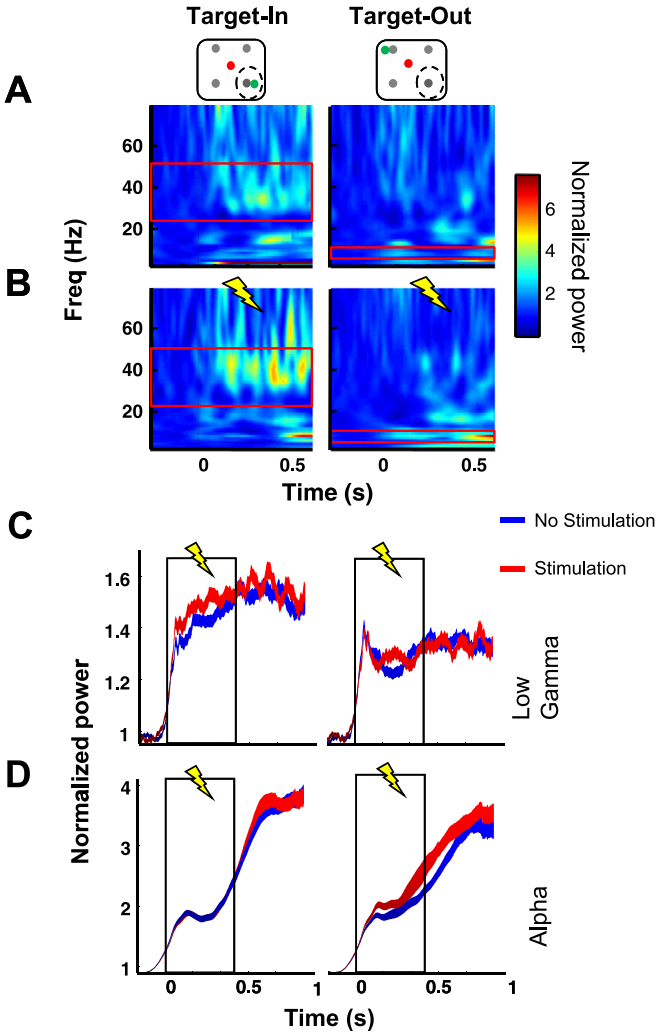

Fig. 2. Effect of FEF microstimulation on the local field potential (LFP) power in LIP. *A* and *B*: example site. *A*: time-frequency plot of the LFP power for the conditions without FEF stimulation (*left*: Target-In trials, *right*: Target-Out trials). *B*: time-frequency plot of the LFP power during FEF microstimulation. Vertical black lines represent stimulus and FEF stimulation onset. *Left*: Target-In conditions. *Right*: Target-Out conditions. *C*: average low-gamma power over all recording sites plotted as a function of time after stimulus onset. Black boxes demarcate the stimulation interval. Blue, no-stimulation trials; red, stimulation trials. *Left*: Target-In conditions. *Right*: Target-Out conditions. *D*: average alpha power as a function of time after stimulus onset for Target-In (*left*) and Target-Out (*right*) trials. Same conventions as in *C*.

in which the saccade target and distractor appeared inside the RF (Target-In trials) than in trials in which only a distractor appeared in the RF (Target-Out trials) [high gamma (120–170 Hz), medium-gamma (50–80 Hz) and low-gamma (25–50 Hz): permutation test; 0–500 ms; $P < 0.001$, Fig. 2*A*; for the differences between the gamma bands see Ray and Maunsell 2011]. Importantly, FEF microstimulation caused an additional increase in low-gamma power in Target-In trials (Fig. 2*B*, *left*, marked in red) but not in Target-Out trials. In contrast, FEF microstimulation caused a significant increase in alpha power (8–12 Hz) in Target-Out trials (Fig. 2*B*, *right*, red box) but not in Target-In trials. Target-In and Target-Out trials differed in the amount of stimuli presented in the RF: during Target-In trials a target and a distractor appeared in the RF, while only one distractor was presented in Target-Out trials. Previous studies have shown, however, that when a saccade target is presented inside the RF, adding a distractor in the RF does not affect LIP spike rate or LFP activity (Janssen and Shadlen 2005; Premereur et al. 2012). It is therefore unlikely that the highly condition-specific effects of FEF microstimulation were merely due to the difference in visual stimulation of the RF in both conditions.

Since the effects of weak FEF microstimulation on the LFP power in area LIP were rarely significant for individual recording sites (permutation test, $P < 0.05$; low gamma: $N = 4/86$, alpha: $N = 7/86$), we averaged the power over frequencies for every frequency band and pooled the data of the two monkeys. The lack of effects on individual recording sites was most likely due to the relatively low number of trials per recording site (on average 141 trials). Averaged across all our recording sites, electrical microstimulation of FEF during Target-In trials caused a significant increase in low-gamma power in the interval (0–500 ms) after target onset (permutation test, $P < 0.05$ for both monkeys) compared with no-stimulation trials (Fig. 2*C*, *left*). The average LIP low-gamma response in the absence of FEF microstimulation (+40% compared with prestimulus baseline) rose by 7–10% during FEF microstimulation, a relative increase of 18–25%. In contrast, FEF microstimulation elicited no significant increase in the low-gamma power in LIP in the interleaved Target-Out trials ($P = 0.41$, Fig. 2*C*, *right*; interaction between target position and FEF microstimulation $P = 0.05$, ANOVA; $F = 3.83$, df = 1). The selectivity of the FEF microstimulation effect for Target-In trials excluded the possibility that the increase in power was a mere artifact of electrical stimulation. The results were significant in both monkeys individually (Fig. 3; permutation test, *monkey Tb*: $P = 0.03$; *monkey Tm*: $P = 0.01$). Figure 3 also shows that the effects of FEF microstimulation on LIP gamma power are not limited to one frequency but are present throughout the entire low-gamma frequency. Furthermore, the effect does not spread to higher or lower frequencies. Most of the FEF saccade vectors in our experiments were directed toward the upper visual field (Fig. 1*B*), but the observation of a significant effect in both monkeys argues against the possibility of an idiosyncratic effect related to the stimulation of particular FEF clusters.

The selective increase in low-gamma power caused by FEF microstimulation started shortly after stimulation onset (52 ms, permutation test, $P < 0.002$ uncorrected for multiple comparisons over bins), was significant up to 388 ms after stimulation onset ($P > 0.05$ in every 1-ms bin between 388 and 500 ms), and disappeared shortly after the stimulation epoch ($P = 0.24$ for the interval 500–700 ms). The enhancement of low-gamma power caused by FEF microstimulation did not correlate with the strength of the LIP low-gamma response ($r = 0.19$, $P = 0.07$ for Target-In trials; $r = 0.11$, $P = 0.16$ for both Target-In and Target-Out trials). Although the effect of FEF microstimulation was not significant for the entire stimulation interval, it did produce a very transient increase in low-gamma power when the saccade was planned away from the RF [$P < 0.002$ in the interval (285–299 ms); Fig. 2*C*, *right*].

In the absence of FEF microstimulation, the low-gamma power in LIP first started to signal the presence of the saccade target in the LIP RF around 155 ms after stimulus onset (permutation test on the difference between Target-In and Target-Out trials, $P < 0.002$ uncorrected for multiple comparisons). However, during FEF stimulation the difference in the

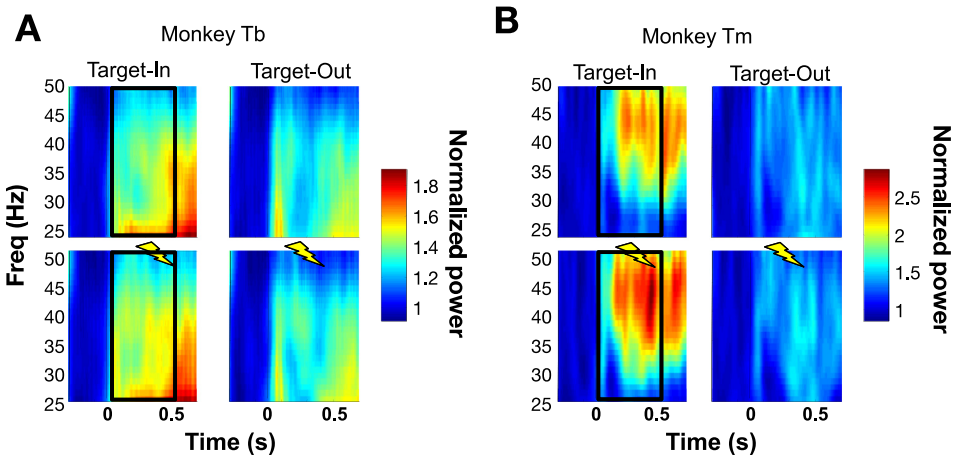

Fig. 3. Normalized low-gamma power. *A*: *monkey Tb*. *B*: *monkey Tm*. Power is plotted as a function of time after stimulus onset (*time 0*) for trials without (*top*) and with (*bottom*) FEF microstimulation. *Left*: Target-in trials. *Right*: Target-out trials. The effect of FEF microstimulation on the low-gamma power was significant in both monkeys (compare values in black squares).

low-gamma powers of Target-In and Target-Out trials emerged as early as 52 ms after stimulus onset ($P < 0.002$ uncorrected). Thus the FEF-induced increase in LIP low-gamma power accelerated the detection of the target location in the gamma band by 100 ms.

FEF microstimulation also caused a significant increase in power of the alpha band, but in contrast to the effect on the low-gamma band, alpha power increased only in Target-Out trials (Fig. 2*D*; permutation test, 0–500 ms: Target-In: $P = 0.60$, Target-Out: $P = 0.02$; *monkey Tm*: +12.34%, $P = 0.14$; *monkey Tb*: +9.65%, $P < 0.03$). Even after the 500-ms period of FEF stimulation, the alpha power remained temporarily elevated (Fig. 2*D*, *right*, 500–700 ms: $P < 0.01$). As was the case for the increase in low-gamma power, the modulation of alpha power started shortly after stimulation onset (57 ms, $P < 0.002$). Across our recording sites the FEF-induced increase in low-gamma power for Target-In trials did not correlate with the FEF-induced increase in alpha power for Target-Out trials ($r = -0.06$, not significant). FEF stimulation did not cause any significant changes in other frequency bands (0–500 ms: $P > 0.05$).

We also recorded LIP SUA during FEF microstimulation in a subset of the recording sites (*monkey Tm*: $N = 20$, *monkey Tb*: $N = 33$). (MUA could not be analyzed because the artifact removal method could not be employed for small spike waveforms; see MATERIALS AND METHODS.) We did not observe any significant effect of FEF microstimulation on the LIP SUA during the microstimulation epoch (data not shown). Similarly, in the epoch after microstimulation (520–840 ms after stimulus onset) the number of recording sites significantly affected by FEF microstimulation (4/86 SUA and MUA combined, Target-in condition) was not higher than expected by chance. Figure 4*A* shows that the distribution of the modulation index (STIM − NOSTIM)/(STIM + NOSTIM) for all recording

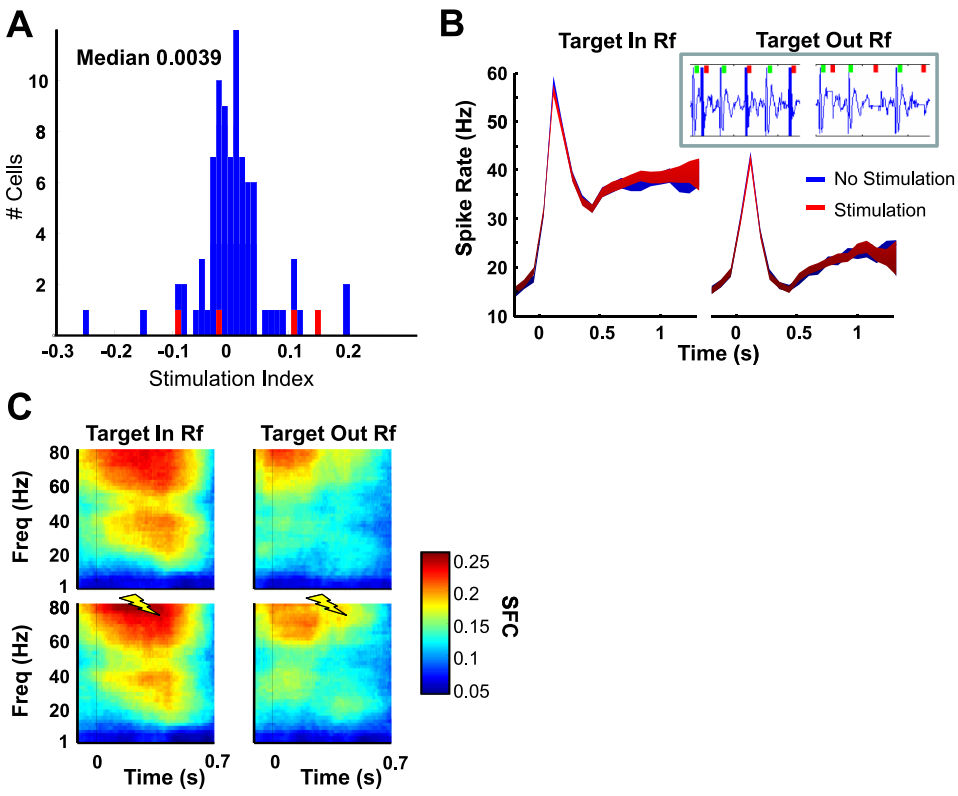

Fig. 4. Stimulation indexes, average single-unit activity, and spike-field coherence (SFC) in LIP. *A*: distribution of stimulation indexes calculated in the interval 520–840 ms. Cells with a significant effect are shown in red. *B*: average LIP spike rate plotted as a function of time after stimulus onset for Target-In (*left*) and Target-Out (*right*) conditions separately for stimulation (red) and no-stimulation (blue) trials. *Inset*, *left*: part of the neural signal recorded during FEF stimulation. Spikes are marked with green lines and stimulation pulses with red lines. *Right*: the neural signal after artifact removal. *C*: SFC in LIP plotted as a function of time after stimulus onset. *Top*: coherence in the absence of FEF-microstimulation for Target-In (*left*) and Target-Out (*right*) trials. *Bottom*: average SFC in LIP during FEF microstimulation.

sites ($N = 53$ SUA and $N = 33$ MUA) in the Target-in condition is centered at zero (median stimulation index = 0.004). Although subthreshold stimulation of FEF also significantly affected low-gamma power during Target-In trials for the subset of SUA recording sites (permutation test, $P < 0.05$), we found no effect on average LIP SUA, either during (*t*-test, $P > 0.73$) or after (500–800 ms: $P > 0.71$) FEF microstimulation, in both Target-In and Target-Out trials (Fig. 4*B*). Note that the artifact removal method (Fig. 4*B*, *inset*) leads to an underestimation of the real spike rate during the stimulation interval (0–500 ms) by ~20%, which explains the "rebound" in the spike rate around 500 ms. Moreover, FEF microstimulation did not have any significant effect on the RT of the monkeys (*t*-test, $P > 0.05$), most likely because microstimulation ceased before the go signal appeared in even the shortest trials (in 93% of trials the go signal appeared later than 700 ms after target onset and thus 200 ms after the stimulation epoch). Furthermore, FEF stimulation had no effect on the monkeys' accuracy, eye velocity, or number of microsaccades. Thus weak electrical microstimulation of FEF selectively affected the LFP power in area LIP but not the LIP spike rate or the subject's behavior.

To determine whether FEF microstimulation caused LIP neurons to fire more in synchrony with the (low gamma) oscillations of the LFP, we calculated the SFC between the spikes and the LFP recorded on the same electrode in LIP (Fig. 4*C*). The SFC in the gamma band—but not in the lower frequencies—was transiently elevated (100–300 ms) after stimulus onset, and more so for Target-In trials than for Target-Out trials (compare Fig. 4*C*, *top left* and *right*; permutation test, $P < 0.05$), but we observed no effect of FEF microstimulation on the SFC in any frequency band ($P > 0.3$; Fig. 4*C*, *bottom*). These results suggest that the effect of weak electrical microstimulation of FEF was largely limited to the input and local processing level of LIP, which are measured in the LFP, but did not influence the output of LIP as no effect was obtained on average LIP spike rate or on SFC.

In all previous experiments we selected an FEF electrode that evoked an eye movement in the direction of the center of the LIP RF, as determined in a manual mapping procedure. Since the lack of any FEF microstimulation effects on LIP SUA might be due to imperfect alignment of the LIP RF and the FEF saccade vector, we systematically mapped the LIP RF for a subset of the recording sites ($N = 60$) by measuring the LIP responses to visually guided saccades in 10 different directions and then plotted the FEF saccade vector on the RF map (RF-mapping task; Fig. 5*A*). Generally, LIP neurons responded most strongly to a saccade target positioned in the upper right position in the visual field, and the average FEF saccade vector was also directed toward the upper right position (see also Fig. 1*B*, 4th panel; in both monkeys the FEF electrodes eliciting saccades toward the upper contralateral visual field proved to be the most reliable). The Euclidean distance between the end point of the saccade vector and the position in the RF-mapping task evoking the maximum response (which did not always correspond to the position in the visual field evoking the maximum response) averaged 5.7°, whereas the average LIP RF size was 37°[2]. Furthermore, the interpolated spike rate at the end point of the saccade vector averaged 83% of the maximum spike rate obtained in the RF-mapping task. These results indicate that the FEF saccade vector was well aligned with the LIP RF, which makes it unlikely that the lack of SUA effects could be explained by imperfect alignment of the FEF saccade vector and LIP RF.

To investigate the spatial specificity of FEF microstimulation, we also recorded at LIP sites in which the RF was not aligned with the FEF saccade vector (*monkey Tm*: $N = 13$, *monkey Tb*: $N = 22$; average Euclidean distance between the maximum of the RF-mapping task and the saccade vector: 12.51°; average interpolated spike rate at the saccade vector position was 37.15% of the maximum spike rate obtained in the RF-mapping task; Fig. 5*B*). Under these conditions, FEF stimulation did not have a significant effect on the LIP low-gamma power (permutation test, Target-In RF: $P = 0.73$, Target-Out RF: $P = 0.13$; Fig. 6*A*), alpha power (Target-In RF: $P = 0.38$, Target-Out RF: $P = 0.09$), or any other frequency band. Thus FEF microstimulation caused significant modulations only in low-gamma and alpha power when the FEF saccade vector was aligned with the LIP RF. The lack of effects in the control task, together with the condition specificity in the experimental sessions, indicates that the effects of FEF microstimulation were not idiosyncratic to the particular FEF electrodes used in our experiments, especially because similar FEF electrodes were used in both the experimental and

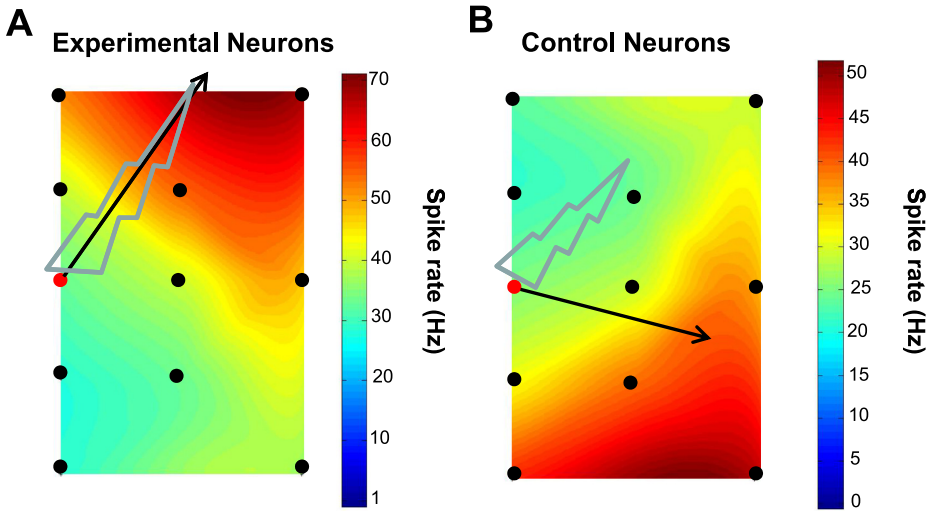

Fig. 5. Average RF maps. *A*: experimental neurons ($N = 60$). *B*: control neurons ($N = 26$). Colors show the average interpolated spike rate for 10 saccade-target positions in the contralateral hemifield (black dots). The red dot is the fixation point. The average position of the target in the Target-In condition of the microstimulation experiment is marked by the black arrows; the average end point of the saccade vector is marked by the tip of the lightning symbol.

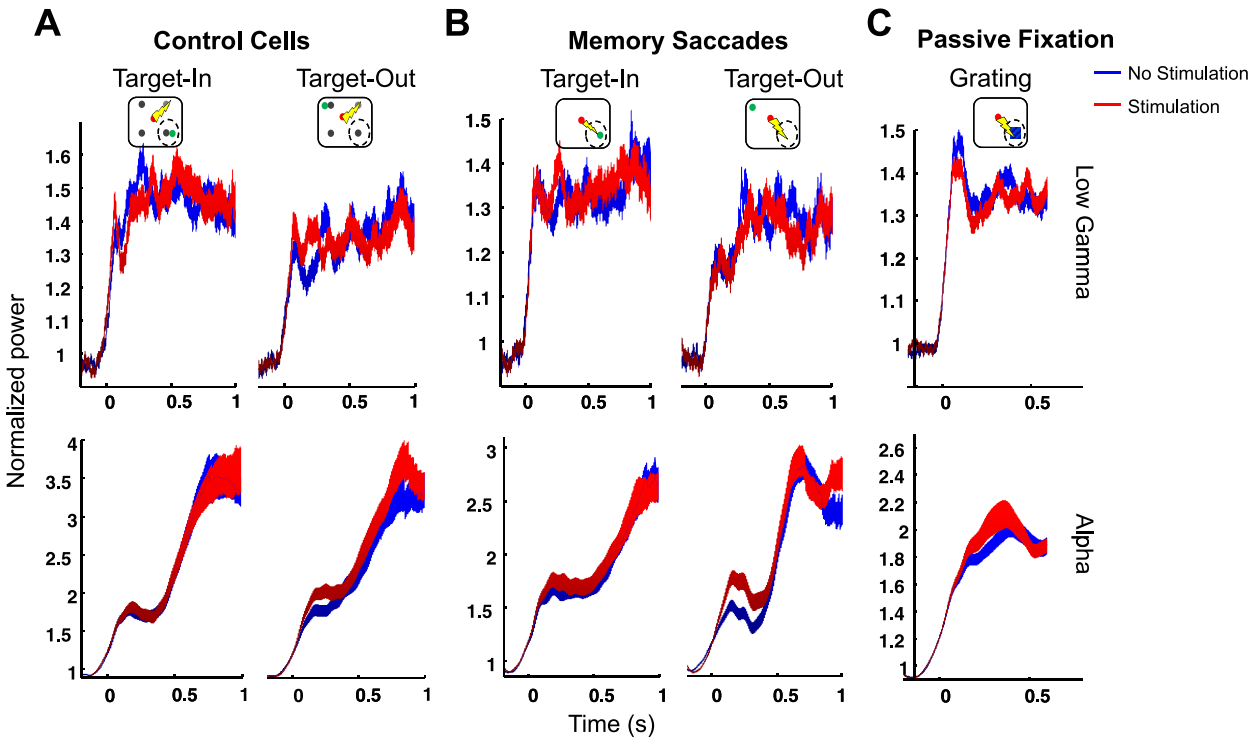

Fig. 6. Control experiments. Average low-gamma power (*top*) and average alpha power (*bottom*) as a function of time after stimulus onset (*time 0*). Stimulation conditions are shown in red and no-stimulation conditions in blue. Shaded area represents SE. *A*: average LFP power in control cells ($N = 35$), in which the LIP RF was not aligned with the FEF saccade vector. The target was either positioned inside the LIP RF (*left*) or in the opposite visual field (*right*) *B*: average LFP power during memory-guided saccades ($N = 59$), with the target appearing briefly either inside the RF (*left*) or in the opposite visual field (*right*). *C*: average LFP power during passive fixation ($N = 62$) with a grating appearing in the RF.

control sessions (see Fig. 1*B*, 4th panel; compare red and blue dots).

Because we wanted to assess the task specificity of the FEF microstimulation effects on LIP, we also employed a memory saccade task ($N = 59$) and a passive fixation task ($N = 62$) in a subset of the recording sites tested with the visually guided saccade task. FEF microstimulation elicited no significant effects on LIP low-gamma power during memory-guided saccades, either in Target-In trials ($P = 0.42$) or in Target-Out trials ($P = 0.69$; Fig. 6*B*). However, during memory-guided saccades, FEF microstimulation significantly increased LIP alpha power when saccades were directed away from the RF (permutation test, Target-In: $P = 0.20$; Target-Out: $P < 0.01$). The increase in alpha power during memory saccades evoked by FEF stimulation did not persist beyond the stimulation interval, suggesting that the continuous presence of a salient stimulus in the visual field (even on the ipsilateral side) was necessary for the FEF microstimulation effect on the alpha power. Finally, no effects of FEF microstimulation were observed in the passive fixation task in which a grating appeared in the RF (Fig. 6*C*). Thus the effect of FEF microstimulation on LIP was not only spatially specific (i.e., only when the LIP RF was aligned with the FEF saccade vector) and frequency specific but also task specific: FEF enhanced low-gamma power in LIP during visually guided saccades when the saccade target remained present in the LIP RF but not during memory-guided saccades or during passive fixation. The effects of FEF microstimulation on alpha power appeared less task specific and were invariably observed when saccades were directed away from the RF.

Because the stimulation parameters we employed (1/3 of the saccade threshold, 100 Hz, pulse width = 0.16 ms) were much weaker than those used in earlier fMRI experiments [1/2 of the saccade threshold, pulse width = 0.48 ms; 335 Hz (Ekstrom et al. 2008, 2009)], our results do not allow the direct comparison of single-cell activity with the fMRI activations in LIP resulting from FEF microstimulation. Moreover, in a separate fMRI experiment we observed LIP activations in both monkeys when we stimulated FEF with the parameters of Ekstrom et al. (2008) but not with the weaker stimulation pulses used in the present experiment.

DISCUSSION

FEF microstimulation evoked significant and highly task- and frequency-specific effects on the LFP power in LIP but not on LIP spike rate or the animals' behavior. FEF stimulation enhanced low-gamma power for saccades toward the RF in retinotopically matched clusters of LIP neurons and increased alpha oscillations for saccades away from the LIP RF.

The lack of any FEF-induced spike rate effects in LIP can be explained by the weak stimulation parameters we had to use in order to measure the effect of FEF microstimulation during the microstimulation epoch. In fact, LIP neurons can be orthodromically activated after FEF stimulation with strong currents (on average 600 μA) (Ferraina et al. 2002). The increased gamma activity we measured in LIP suggests that at least some LIP neurons were affected by FEF stimulation. It is important to note that we recorded mostly from large (putative excitatory) neurons. The effect of FEF stimulation may be more visible in inhibitory interneurons (Cardin et al. 2009), similar to the

effect of spatial attention, which is mostly present in small interneurons (Mitchell et al. 2007).

Distinguishing between orthodromic and antidromic effects represents a thorny problem for most microstimulation studies (Moeller et al. 2008; Moore and Armstrong 2003). An antidromic account of our results would build on the assumption that Target-in trials activate a set of (possibly inhibitory) neurons (Cardin et al. 2009; Sohal et al. 2009) in LIP that project to FEF: these LIP neurons would induce a gamma rhythm during Target-in trials, which would be antidromically enhanced by FEF microstimulation. In all likelihood, an antidromic activation of LIP neurons would also enhance gamma power in a variety of tasks, which is not what we observed. An orthodromic interpretation of our effects, on the other hand, would encompass FEF fibers projecting to retinotopically matched sites in LIP, which would induce gamma oscillations in LIP (possibly through inhibitory interneurons) during Target-in trials and then further enhance this elevated gamma rhythm during FEF microstimulation. Assuming that the LFP represents mainly synaptic input and local processing activity, the enhancement of gamma power caused by FEF stimulation is more compatible with an orthodromic effect. However, given the strong reciprocal connections between LIP and FEF, our microstimulation may have evoked both orthodromic and antidromic activation of LIP neurons. Future studies investigating the neural basis of gamma oscillations in area LIP are needed to clarify this problem.

Previous studies have investigated the importance of different stimulation parameters for eliciting saccades. Tehovnik and Sommer (1997) tested a range of frequencies and pulse durations and showed that for frequencies between 100 and 1,000 Hz the probability for evoking a saccade remained at 100% (using 400-μA current, 0.1-ms pulse duration and 400-ms train duration). Furthermore, the authors showed that, although the current thresholds change with more narrow pulses, saccades could still be evoked. To date, however, no study has investigated the importance of stimulation parameters in evoking attention effects. The stimulation parameters we employed (100 Hz, 0.16-ms pulse width) were sufficient to evoke saccades, but stimulating at one-third of the threshold did not produce reliable behavioral effects. Note, however, that the timing of our stimulation parameters was not optimal for causing behavioral effects (see Moore and Fallah 2004). Rather than exploring a range of stimulation parameters, we focused on the effect of FEF microstimulation on LIP in different tasks (visually guided and memory-guided saccade tasks and passive fixation). We observed increases in two different frequency bands (low gamma for Target-In trials and alpha power for Target-Out trials), which argues against the possibility that the LFP effects were tied to particular frequency bands because of the stimulation frequency we chose. The lack of any significant effect on behavior was likely caused by the fact that 93% of trials ended at least 200 ms after microstimulation (0–500 ms) had ceased. Nevertheless, future studies should investigate the effect of subthreshold FEF microstimulation on LIP with different stimulation parameters and in tasks where stimulus detection closely coincides with the microstimulation epoch.

The target selectivity in the low-gamma band (i.e., the difference between Target-In and Target-Out trials) emerged 100 ms earlier in trials with FEF microstimulation than in trials without FEF microstimulation. Hence at a point in time when the low-gamma band in LIP was normally not yet informative about target position (50–155 ms after stimulus onset) FEF microstimulation was already able to differentiate between Target-In and Target-Out trials in the low-gamma power. In our experiments, the start of FEF microstimulation always coincided with stimulus onset, i.e., ~50 ms before the visual latency of the FEF neurons and at least 100 ms before FEF neurons could detect the pop-out target (Bichot and Schall 1999; Thompson et al. 1996). Given the estimated theoretical latency of the FEF microstimulation effect on LIP low-gamma power (1 cycle: ~50 ms), the first 50 ms of FEF stimulation must have already initiated the early increase in LIP low-gamma power (50–100 ms after stimulus onset) that was selective for target location. However, the spike rates of LIP neurons signal the presence of pop-out stimuli at very short latencies (50 ms) (Buschman and Miller 2007; Premereur et al. 2011), much faster than the FEF does (Bichot and Schall 1999; Schall et al. 2007). Therefore the remarkably early target-selective gamma enhancement in LIP most likely reflects an interaction between top-down signals from the FEF and bottom-up target detection by LIP neurons.

The functional role of gamma oscillations in visual cortex is heavily debated at present (Fries et al. 2001; Ray and Maunsell 2011), but only a few studies have measured LFPs in area LIP. Elevated and sustained gamma activity is observed during memory-guided saccades toward the RF in a population of LIP neurons with high memory-delay activity (Pesaran et al. 2002). Moreover, during pop-out the FEF-LIP coherence is specifically elevated in the gamma band, whereas during visual search the FEF-LIP coherence occurs in the beta band (Buschman and Miller 2007). Our saccade task can be compared with a typical pop-out task in that the saccade target differed from the four distractors by its color. In view of the difference in the latencies of pop-out detection in FEF and LIP, fast, bottom-up target selection during pop-out may occur first in LIP, whereas the longer-latency top-down target selection during visual search may emerge first in the frontal cortex (Buschman and Miller 2007). Intriguingly, in our pop-out task we observed FEF-induced enhancement of the gamma power within the same frequency range as that of the FEF-LIP coherence (Buschman and Miller 2007). Thus the influence of FEF on LIP during pop-out appears to be specifically tied to the low-gamma band when a salient saccade target appears in the RF. Future studies will have to determine whether the FEF would influence other frequency bands (e.g., beta) in LIP during visual search.

We have demonstrated low-gamma responses in LIP without visual RF stimulation associated with the temporal expectation of stimulus onset (Premereur et al. 2012). The low-gamma response in LIP was significantly larger in Target-In trials of the multiple-distractor task compared with trials without visual stimulation but not in Target-Out trials, memory saccades, or passive fixation. Here we have shown that FEF microstimulation additionally enhances this elevated low-gamma response for Target-In trials but not during memory saccades or passive fixation. Therefore the effect of FEF microstimulation was not associated with planning and executing eye movements toward the RF per se (memory saccades) or with the appearance of salient stimuli in the RF (grating): FEF microstimulation primarily induced gamma oscillations in LIP when that salient stimulus was the target for a saccade.

The saccade target was highly salient because it differed from the four (identical) distractors by its color, thereby automatically drawing attention (Desimone and Duncan 1995). Furthermore, the attentional priority resides primarily at the location of the saccade target in a delayed-saccade task (Bisley and Goldberg 2003, 2006). We have previously demonstrated that that LIP gamma power is elevated for salient stimuli in the RF (Premereur et al. 2012), similar to other extrastriate areas (Fries et al. 2001; Khayat et al. 2010). Thus our results suggest that the FEF can enhance the attentional priority of saccade targets at retinotopically matched locations in LIP, at least at the level of the LFP. Since the enhanced gamma synchronization in area V4 with attention may also be initiated by the FEF (Gregoriou et al. 2009), our results suggest that the FEFs exert a widespread influence on more posterior visual areas when directing attention.

We also observed a very transient increase in low-gamma power in Target-out trials evoked by FEF microstimulation in the middle of the stimulation epoch. If our attentional interpretation of the FEF effect is correct, this transient enhancement may be similar to the shift in attentional priority evoked by a flashed distractor in the RF (Bisley and Goldberg 2003).

FEF microstimulation can enhance visual responses in retinotopically corresponding sites and suppress responses at noncorresponding locations (Moore and Armstrong 2003), similar to the known effects of selective attention. Imaging studies have also presented evidence favoring a push-pull mechanism for directing selective attention controlled by a frontoparietal network (Pinsk et al. 2004). We observed robust alpha responses in LIP that were not specific for target location (inside or outside the RF) or task (saccades or passive fixation) in trials without FEF microstimulation and an FEF-induced increase in alpha power for saccades directed away from the LIP RF. Alpha oscillations in visual cortex have been associated with stimulus anticipation, disengagement of spatial attention (Thut et al. 2006), reduction in cortical excitability (Klimesch et al. 2007), and inhibition of unattended stimuli (Haegens et al. 2011; Klimesch et al. 2007). Taken together, our data are at least consistent with the hypothesis that the FEF exerts a push-pull influence on clusters of LIP neurons, possibly by increasing cortical excitability (low gamma) when targets appear in the RF and decreasing cortical excitability (alpha) when distractors appear in the RF. Note, however, that we did not observe a corresponding decrease in alpha power in Target-In trials, as one would expect if gamma and alpha power were to act in a symmetrical push-pull arrangement. At least in our experiments FEF microstimulation evoked task-dependent increases in LFP power but no decreases in LFP power.

Does FEF also influence gamma oscillations in LIP in natural behavior during pop-out? Such an experiment would require reversible inactivation of FEF combined with LIP recordings during pop-out. However, FEF inactivation causes a profound deficit in attention (both conjunction search and pop-out) and saccadic behavior (Wardak et al. 2006), which would make the interpretation of any effect of FEF inactivation on LIP during saccade tasks problematic. The fact that FEF microstimulation did not disrupt the dynamics of the low-gamma in LIP (i.e., almost parallel upward shift in the low-gamma power) constitutes indirect support for the hypothesis that the effect of FEF microstimulation on LIP was similar to what may occur in natural conditions.

ACKNOWLEDGMENTS

We thank Stijn Verstraeten, Piet Kayenbergh, Gerrit Meulemans, Marc De Paep, Inez Puttemans, and Marjan Docx for assistance and Steve Raiguel for comments on a previous version of this manuscript.

GRANTS

This work was supported by Geneeskundige Stichting Koningin Elisabeth, Fonds voor Wetenschappelijk Onderzoek (G.0713.09, G.0622.08, and G.0831.11), National Science Foundation (NSF) Grant BCS-0745436, Interuniversity Attraction Poles (P6/29), Excellentie Financiering (EF/05/014), Programma Financiering (PFV/10/008), and Geconcerteerde onderzoeksacties (GOA/10/19).

DISCLOSURES

No conflicts of interest, financial or otherwise, are declared by the author(s).

AUTHOR CONTRIBUTIONS

Author contributions: E.P., W.V., P.R.R., and P.J. conception and design of research; E.P. performed experiments; E.P. analyzed data; E.P., W.V., P.R.R., and P.J. interpreted results of experiments; E.P. prepared figures; E.P. drafted manuscript; E.P., W.V., P.R.R., and P.J. edited and revised manuscript; E.P., W.V., P.R.R., and P.J. approved final version of manuscript.

REFERENCES

Anderson JC, Kennedy H, Martin KA. Pathways of attention: synaptic relationships of frontal eye field to V4, lateral intraparietal cortex, and area 46 in macaque monkey. *J Neurosci* 31: 10872–10881, 2011.

Bichot NP, Schall JD. Effects of similarity and history on neural mechanisms of visual selection. *Nat Neurosci* 2: 549–554, 1999.

Bisley JW, Goldberg ME. Neuronal activity in the lateral intraparietal area and spatial attention. *Science* 299: 81–86, 2003.

Bisley JW, Goldberg ME. Neural correlates of attention and distractibility in the lateral intraparietal area. *J Neurophysiol* 95: 1696–1717, 2006.

Bokil H, Andrews P, Kulkarni JE, Mehta S, Mitra PP. Chronux: a platform for analyzing neural signals. *J Neurosci Methods* 192: 146–151, 2010.

Bruce CJ, Goldberg ME, Bushnell MC, Stanton GB. Primate frontal eye fields. II. Physiological and anatomical correlates of electrically evoked eye movements. *J Neurophysiol* 54: 714–734, 1985.

Buschman TJ, Miller EK. Top-down versus bottom-up control of attention in the prefrontal and posterior parietal cortices. *Science* 315: 1860–1862, 2007.

Cardin JA, Carlen M, Meletis K, Knoblich U, Zhang F, Deisseroth K, Tsai LH, Moore CI. Driving fast-spiking cells induces gamma rhythm and controls sensory responses. *Nature* 459: 663–667, 2009.

Colby CL, Duhamel JR, Goldberg ME. Visual, presaccadic, and cognitive activation of single neurons in monkey lateral intraparietal area. *J Neurophysiol* 76: 2841–2852, 1996.

Corbetta M, Akbudak E, Conturo TE, Snyder AZ, Ollinger JM, Drury HA, Linenweber MR, Petersen SE, Raichle ME, Van E, Shulman GL. A common network of functional areas for attention and eye movements. *Neuron* 21: 761–773, 1998.

Desimone R, Duncan J. Neural mechanisms of selective visual attention. *Annu Rev Neurosci* 18: 193–222, 1995.

Ekstrom LB, Roelfsema PR, Arsenault JT, Bonmassar G, Vanduffel W. Bottom-up dependent gating of frontal signals in early visual cortex. *Science* 321: 414–417, 2008.

Ekstrom LB, Roelfsema PR, Arsenault JT, Kolster H, Vanduffel W. Modulation of the contrast response function by electrical microstimulation of the macaque frontal eye field. *J Neurosci* 29: 10683–10694, 2009.

Ferraina S, Pare M, Wurtz RH. Comparison of cortico-cortical and cortico-collicular signals for the generation of saccadic eye movements. *J Neurophysiol* 87: 845–858, 2002.

Fries P, Reynolds JH, Rorie AE, Desimone R. Modulation of oscillatory neuronal synchronization by selective visual attention. *Science* 291: 1560–1563, 2001.

Gattass R, Desimone R. Responses of cells in the superior colliculus during performance of a spatial attention task in the macaque. *Rev Bras Biol* 56: 257–279, 1996.

Gregoriou GG, Gotts SJ, Zhou H, Desimone R. High-frequency, long-range coupling between prefrontal and visual cortex during attention. *Science* 324: 1207–1210, 2009.

Haegens S, Handel BF, Jensen O. Top-down controlled alpha band activity in somatosensory areas determines behavioral performance in a discrimination task. *J Neurosci* 31: 5197–5204, 2011.

Huerta MF, Krubitzer LA, Kaas JH. Frontal eye field as defined by intracortical microstimulation in squirrel monkeys, owl monkeys, and macaque monkeys. II. Cortical connections. *J Comp Neurol* 265: 332–361, 1987.

Janssen P, Shadlen MN. A representation of the hazard rate of elapsed time in macaque area LIP. *Nat Neurosci* 8: 234–241, 2005.

Khayat PS, Niebergall R, Martinez-Trujillo JC. Frequency-dependent attentional modulation of local field potential signals in macaque area MT. *J Neurosci* 30: 7037–7048, 2010.

Klimesch W, Sauseng P, Hanslmayr S. EEG alpha oscillations: the inhibition-timing hypothesis. *Brain Res Rev* 53: 63–88, 2007.

Kustov AA, Robinson DL. Shared neural control of attentional shifts and eye movements. *Nature* 384: 74–77, 1996.

Liu Y, Yttri EA, Snyder LH. Intention and attention: different functional roles for LIPd and LIPv. *Nat Neurosci* 13: 495–500, 2010.

Mitchell JF, Sundberg KA, Reynolds JH. Differential attention-dependent response modulation across cell classes in macaque visual area V4. *Neuron* 55: 131–141, 2007.

Moeller S, Freiwald WA, Tsao DY. Patches with links: a unified system for processing faces in the macaque temporal lobe. *Science* 320: 1355–1359, 2008.

Moore T, Armstrong KM. Selective gating of visual signals by microstimulation of frontal cortex. *Nature* 421: 370–373, 2003.

Moore T, Fallah M. Control of eye movements and spatial attention. *Proc Natl Acad Sci USA* 98: 1273–1276, 2001.

Moore T, Fallah M. Microstimulation of the frontal eye field and its effects on covert spatial attention. *J Neurophysiol* 91: 152–162, 2004.

Nobre AC, Gitelman DR, Dias EC, Mesulam MM. Covert visual spatial orienting and saccades: overlapping neural systems. *Neuroimage* 11: 210–216, 2000.

Pesaran B, Pezaris JS, Sahani M, Mitra PP, Andersen RA. Temporal structure in neuronal activity during working memory in macaque parietal cortex. *Nat Neurosci* 5: 805–811, 2002.

Petersen SE, Robinson DL, Morris JD. Contributions of the pulvinar to visual spatial attention. *Neuropsychologia* 25: 97–105, 1987.

Pinsk MA, Doniger GM, Kastner S. Push-pull mechanism of selective attention in human extrastriate cortex. *J Neurophysiol* 92: 622–629, 2004.

Premereur E, Vanduffel W, Janssen P. Functional heterogeneity of macaque lateral intraparietal neurons. *J Neurosci* 31: 12307–12317, 2011.

Premereur E, Vanduffel W, Janssen P. Local field potential activity associated with temporal expectations in the macaque lateral intraparietal area. *J Cogn Neurosci* 24: 1314–1330, 2012.

Ray S, Maunsell JH. Different origins of gamma rhythm and high-gamma activity in macaque visual cortex. *PLoS Biol* 9: e1000610, 2011.

Reynolds JH, Chelazzi L. Attentional modulation of visual processing. *Annu Rev Neurosci* 27: 611–647, 2004.

Reynolds JH, Chelazzi L, Desimone R. Competitive mechanisms subserve attention in macaque areas V2 and V4. *J Neurosci* 19: 1736–1753, 1999.

Rizzolatti G, Riggio L, Dascola I, Umilta C. Reorienting attention across the horizontal and vertical meridians: evidence in favor of a premotor theory of attention. *Neuropsychologia* 25: 31–40, 1987.

Schall JD. Neural basis of saccade target selection. *Rev Neurosci* 6: 63–85, 1995.

Schall JD, Morel A, King DJ, Bullier J. Topography of visual cortex connections with frontal eye field in macaque: convergence and segregation of processing streams. *J Neurosci* 15: 4464–4487, 1995.

Schall JD, Pare M, Woodman GF. Comment on "Top-down versus bottom-up control of attention in the prefrontal and posterior parietal cortices." *Science* 318: 44, 2007.

Sinkkonen J, Tiitinen H, Naatanen R. Gabor filters: an informative way for analysing event-related brain activity. *J Neurosci Methods* 56: 99–104, 1995.

Sohal VS, Zhang F, Yizhar O, Deisseroth K. Parvalbumin neurons and gamma rhythms enhance cortical circuit performance. *Nature* 459: 698–702, 2009.

Stanton GB, Bruce CJ, Goldberg ME. Topography of projections to posterior cortical areas from the macaque frontal eye fields. *J Comp Neurol* 353: 291–305, 1995.

Stanton GB, Deng SY, Goldberg ME, McMullen NT. Cytoarchitectural characteristic of the frontal eye fields in macaque monkeys. *J Comp Neurol* 282: 415–427, 1989.

Tallon-Baudry C, Bertrand O. Oscillatory gamma activity in humans and its role in object representation. *Trends Cogn Sci* 3: 151–162, 1999.

Tallon-Baudry C, Bertrand O, Delpuech C, Permier J. Oscillatory gamma-band (30–70 Hz) activity induced by a visual search task in humans. *J Neurosci* 17: 722–734, 1997.

Tehovnik EJ, Sommer MA. Electrically evoked saccades from the dorsomedial frontal cortex and frontal eye fields: a parametric evaluation reveals differences between areas. *Exp Brain Res* 117: 369–378, 1997.

Tehovnik EJ, Sommer MA, Chou IH, Slocum WM, Schiller PH. Eye fields in the frontal lobes of primates. *Brain Res Brain Res Rev* 32: 413–448, 2000.

Thier P, Andersen RA. Electrical microstimulation distinguishes distinct saccade-related areas in the posterior parietal cortex. *J Neurophysiol* 80: 1713–1735, 1998.

Thompson KG, Hanes DP, Bichot NP, Schall JD. Perceptual and motor processing stages identified in the activity of macaque frontal eye field neurons during visual search. *J Neurophysiol* 76: 4040–4055, 1996.

Thut G, Nietzel A, Brandt SA, Pascual-Leone A. Alpha-band electroencephalographic activity over occipital cortex indexes visuospatial attention bias and predicts visual target detection. *J Neurosci* 26: 9494–9502, 2006.

Wardak C, Ibos G, Duhamel JR, Olivier E. Contribution of the monkey frontal eye field to covert visual attention. *J Neurosci* 26: 4228–4235, 2006.

Wardak C, Olivier E, Duhamel JR. A deficit in covert attention after parietal cortex inactivation in the monkey. *Neuron* 42: 501–508, 2004.

Wardak C, Vanduffel W, Orban GA. Searching for a salient target involves frontal regions. *Cereb Cortex* 20: 2464–2477, 2010.

Worden MS, Foxe JJ, Wang N, Simpson GV. Anticipatory biasing of visuospatial attention indexed by retinotopically specific alpha-band electroencephalography increases over occipital cortex. *J Neurosci* 20: RC63, 2000.